

## INFLUENCE OF THE $\text{SiN}_x$ DEPOSITION TEMPERATURE ON THE PASSIVATION QUALITY OF $\text{Al}_2\text{O}_3/\text{SiN}_x$ STACKS AND THE EFFECT OF BLISTERING

Yves Patrick Botchak Mouafi, Thomas Lüder, Giso Hahn

University of Konstanz, Department of Physics, 78457 Konstanz, Germany

**Corresponding author:** Yves.Patrick.Botchak@uni-konstanz.de, Tel.: +49 7531 882082, Fax: +49 7531 88 3895

Co-authors: Thomas.Lueder@uni-konstanz.de, Giso.Hahn@uni-konstanz.de

**ABSTRACT:** In this study we investigate the influence of the hydrogen-rich silicon nitride ( $\text{SiN}_x\text{:H}$ ) deposition temperature by a direct PECVD (plasma-enhanced chemical vapour deposition) on the passivation quality of  $\text{Al}_2\text{O}_3/\text{SiN}_x\text{:H}$  stacks and the effect of blister formation on FZ Si material. It is shown that the damage produced by the plasma during deposition of the  $\text{SiN}_x$  coating can be reduced by decreasing the  $\text{SiN}_x\text{:H}$  deposition temperature for a thin  $\text{SiN}_x\text{:H}$  layer of  $\sim 30$  nm. Furthermore, the optical analysis shows that the blistering of the  $\text{Al}_2\text{O}_3/\text{SiN}_x\text{:H}$  stacks after  $\text{SiN}_x\text{:H}$  deposition depends on the deposition temperature and the thickness of the  $\text{SiN}_x\text{:H}$  layer in the case of a direct PECVD. Moreover, the density of blisters seems to be decreased by increasing the  $\text{Al}_2\text{O}_3$  deposition temperature. An annealing step of  $370^\circ\text{C}$  for 40 min under atomic hydrogen atmosphere or under nitrogen atmosphere after  $\text{SiN}_x\text{:H}$  deposition seems to be beneficial for the samples not showing severe blister formation ( $\text{Al}_2\text{O}_3/\text{SiN}_x\text{:H}$  stack with a  $\text{SiN}_x\text{:H}$  layer deposited by direct PECVD at  $300^\circ\text{C}$  or by indirect PECVD at  $400^\circ\text{C}$ ).

**Keywords:** annealing, lifetime, passivation, silicon nitride

### 1 INTRODUCTION

A good passivation of the backside of solar cells gains today in importance with the ever growing industrial onset of PERC (passivated emitter and rear cell) solar cells.  $\text{Al}_2\text{O}_3$  is an appropriate candidate for the passivation of p-type silicon material due to its good chemical surface passivation and its negative fixed charges which yield to a field effect passivation [1]. However, the  $\text{Al}_2\text{O}_3$  layer is not very stable for many solar cells process flows, especially for the high temperature processes, and needs generally to be capped [2]. In this regard the  $\text{SiN}_x\text{:H}$ , which is usually used in the solar cell industry to passivate the front side emitter, seems to be a good candidate. An advantage of  $\text{SiN}_x\text{:H}$  in addition to its chemical stability is its optical contribution to light trapping [3]. Furthermore,  $\text{SiN}_x\text{:H}$  can improve the passivation quality of the  $\text{Al}_2\text{O}_3$  after firing [4]. The most often used method to deposit the  $\text{SiN}_x\text{:H}$  layer is PECVD. However, the use of a direct PECVD causes blistering of the  $\text{Al}_2\text{O}_3/\text{SiN}_x\text{:H}$  stack most probably because of the usual deposition temperature of  $\sim 400^\circ\text{C}$ . Therefore, in this study, we shed light on the influence of  $\text{SiN}_x\text{:H}$  deposition temperatures below  $400^\circ\text{C}$  in case of a direct PECVD on the blistering and the passivation quality of the  $\text{Al}_2\text{O}_3/\text{SiN}_x\text{:H}$  stack on p-type FZ Si wafers.

### 2 EXPERIMENTS

#### 2.1 1<sup>st</sup> experiment

$5 \times 5 \text{ cm}^2$  symmetrical lifetime samples were processed on  $\langle 100 \rangle$  oriented  $\sim 250 \mu\text{m}$  thick p-type FZ silicon wafers of  $\sim 1 \Omega\text{cm}$  resistivity as described in Fig. 1. After etching in a chemical polishing (CP) solution to remove the laser damage at the edges, they were RCA-cleaned. During the last step of the RCA cleaning the chemical oxide was not removed. A thin  $\text{Al}_2\text{O}_3$  layer of  $\sim 7.5$  nm was then deposited on both sides of the wafer at three different substrate set temperatures ( $170^\circ\text{C}$ ,  $200^\circ\text{C}$ , and  $300^\circ\text{C}$ ) using a plasma-assisted atomic layer deposition (ALD) reactor from Oxford Instruments. Subsequently, an  $\text{Al}_2\text{O}_3$  post deposition annealing at  $420^\circ\text{C}$  for 30 min followed to activate the

passivation. The effective minority carrier lifetime  $\tau_{\text{eff}}$  was measured using the photoconductance decay (PCD) method at an injection level of  $1 \times 10^{15} \text{ cm}^{-3}$ . The deposition of a  $\sim 30$  nm  $\text{SiN}_x\text{:H}$  capping layer on both sides of the wafer was then performed using a direct PECVD (Centrotherm) at three different temperatures ( $300^\circ\text{C}$ ,  $350^\circ\text{C}$ , and  $400^\circ\text{C}$ ) and using a remote PECVD (Roth&Rau) at  $400^\circ\text{C}$ . The effective minority carrier lifetime  $\tau_{\text{eff}}$  was once more measured, followed by an annealing at  $370^\circ\text{C}$  for 40 min in atomic hydrogen atmosphere. Finally, another lifetime measurement was performed.

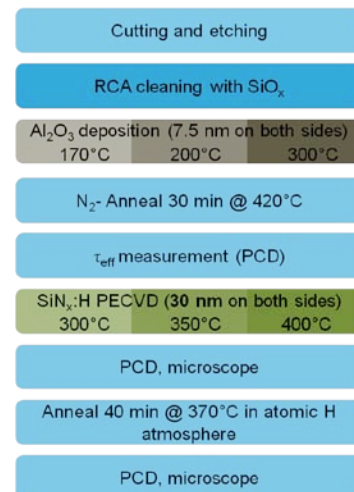


**Figure 1:** Process flow of  $1 \Omega\text{cm}$  p-type FZ lifetime samples. The chemical oxide was not removed after the last step of the RCA cleaning. Passivation was performed by  $\text{Al}_2\text{O}_3$  deposited at three different temperatures ( $170^\circ\text{C}$ ,  $200^\circ\text{C}$  and  $300^\circ\text{C}$ ). The  $\text{SiN}_x\text{:H}$  capping layer of  $\sim 30$  nm was deposited using a direct PECVD at three different temperatures ( $300^\circ\text{C}$ ,  $350^\circ\text{C}$  and  $400^\circ\text{C}$ ) or a remote PECVD at  $400^\circ\text{C}$ .

#### 2.2 2<sup>nd</sup> experiment

To investigate the influence of the thickness of the  $\text{SiN}_x\text{:H}$  layer, a second set of lifetime samples was

processed as illustrated in Fig. 2. In addition, the influence of the chemical oxide and the  $\text{Al}_2\text{O}_3$  post deposition annealing on  $\tau_{\text{eff}}$  and on the blistering phenomenon was examined.

The sample preparation is the same as in the first experiment, except for some process steps and the additional firing step at the end. After the last step of the RCA cleaning the chemical oxide was removed for some samples. Prior to the deposition of the  $\text{SiN}_x\text{:H}$  capping layer, some samples were annealed at  $420^\circ\text{C}$  for 30 min in  $\text{N}_2$  environment, followed by the first  $\tau_{\text{eff}}$  measurement. Thereafter, a thick  $\text{SiN}_x\text{:H}$  capping layer of  $\sim 120$  nm was deposited using a direct PECVD at  $300^\circ\text{C}$  or a remote PECVD at  $400^\circ\text{C}$ . After a second  $\tau_{\text{eff}}$  measurement, an annealing step was carried out not in atomic hydrogen atmosphere, but in nitrogen environment. The third lifetime measurement was performed before a firing step in a belt furnace at  $\sim 850^\circ\text{C}$  preceding another lifetime measurement.

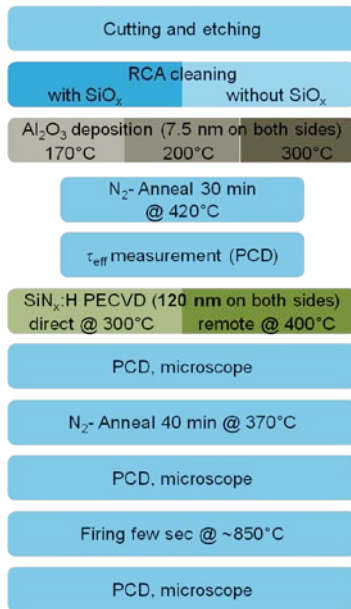


**Figure 2:** Process flow of 1  $\Omega\text{cm}$  p-type FZ lifetime samples. For some samples the chemical oxide was removed after the RCA cleaning. Passivation was carried out by  $\text{Al}_2\text{O}_3$  deposited at three different temperatures ( $170^\circ\text{C}$ ,  $200^\circ\text{C}$  and  $300^\circ\text{C}$ ), subsequently, some samples were annealed before the first  $\tau_{\text{eff}}$  measurement. The  $\text{SiN}_x\text{:H}$  capping layer of  $\sim 120$  nm was deposited using a direct PECVD at  $300^\circ\text{C}$  or a remote PECVD at  $400^\circ\text{C}$ .

### 3 LIFETIME MEASUREMENTS

#### 3.1 1<sup>st</sup> experiment: thin $\text{SiN}_x\text{:H}$ capping layer

The  $\tau_{\text{eff}}$  measurements after the  $\text{Al}_2\text{O}_3$  post-deposition anneal (blue and red squares shown in Fig. 3) reveal that the passivation quality of  $\text{Al}_2\text{O}_3$  depends on the deposition temperature in accordance with previous results [5].

As can be seen in Fig. 3,  $\tau_{\text{eff}}$  is decreased after the  $\text{SiN}_x\text{:H}$  deposition (round symbols) independently of the deposition method and the  $\text{Al}_2\text{O}_3$  deposition temperature. This is probably due to the plasma damage on the  $\text{Al}_2\text{O}_3$  layer or the  $\text{Al}_2\text{O}_3/\text{Si}$  interface, respectively. This was also observed in a similar study [6]. For the direct

PECVD (blue symbols), the plasma damage during  $\text{SiN}_x\text{:H}$  deposition depends strongly on the  $\text{SiN}_x\text{:H}$  deposition temperature and there is a tendency of augmentation with increasing temperature. This can be explained by the fact that during  $\text{SiN}_x\text{:H}$  deposition the velocity of the particles on the substrate surface increases with increasing temperature [9].

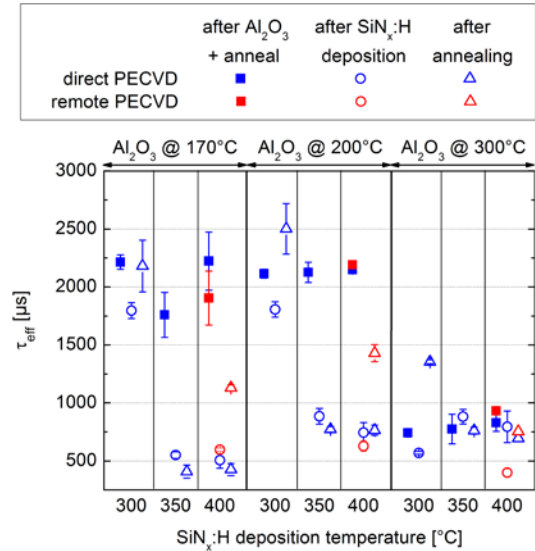


**Figure 3:** Effective minority carrier lifetime  $\tau_{\text{eff}}$  dependant on  $\text{Al}_2\text{O}_3$  and  $\text{SiN}_x\text{:H}$  (direct and remote PECVD) deposition temperature. The  $\text{SiN}_x\text{:H}$  layer thickness is  $\sim 30$  nm. Measurements were carried out after the  $\text{Al}_2\text{O}_3$  post deposition anneal at  $\sim 420^\circ\text{C}$  for 30 min (square), after  $\text{SiN}_x\text{:H}$  deposition (dot) and after an annealing step at  $370^\circ\text{C}$  for 40 min (triangle).

An annealing step at  $370^\circ\text{C}$  for 40 min under 1 mbar atomic hydrogen atmosphere after the  $\text{SiN}_x\text{:H}$  deposition increases  $\tau_{\text{eff}}$  again for the samples which did not show blister formation after the  $\text{SiN}_x\text{:H}$  deposition. This healing of plasma damage by a post-deposition anneal was also found in the aforementioned study [6]. The annealing step was performed in [6] under 10 mbar nitrogen atmosphere. Therefore, the improvement of  $\tau_{\text{eff}}$  after the annealing step is not due to the presence of atomic hydrogen, but seems to be temperature-dependent.

#### 3.2 2<sup>nd</sup> experiment: thick $\text{SiN}_x\text{:H}$ capping layer

Fig. 4 shows  $\tau_{\text{eff}}$  of samples with a chemical oxide after the RCA cleaning (solid symbols) and samples without chemical oxide (empty symbols). The thickness of the  $\text{SiN}_x\text{:H}$  layer is  $\sim 120$  nm. As can be seen in Fig. 4,  $\tau_{\text{eff}}$  is much higher for the samples with a chemical oxide than for the samples without it after the  $\text{Al}_2\text{O}_3$  post deposition anneal (black squares). The plasma damage during the  $\text{SiN}_x\text{:H}$  deposition at  $300^\circ\text{C}$  (direct PECVD) is more pronounced for a thicker  $\text{SiN}_x\text{:H}$  layer ( $\sim 120$  nm) than for a thinner one ( $\sim 30$  nm) (compare red solid circles in Fig. 4 and empty blue circles in Fig. 3 for a  $\text{SiN}_x\text{:H}$  deposition temperature of  $300^\circ\text{C}$ ). The absolute decrease of  $\tau_{\text{eff}}$  after the  $\text{SiN}_x\text{:H}$  deposition is stronger for samples with a chemical oxide in comparison to samples without it, but absolute  $\tau_{\text{eff}}$  values for samples with chemical oxide are mostly higher than values without chemical oxide. On the contrary,  $\tau_{\text{eff}}$  increases (direct PECVD) or is constant (remote PECVD) after the silicon

nitride deposition for the samples without chemical oxide for an  $\text{Al}_2\text{O}_3$  deposition temperature of  $300^\circ\text{C}$ .

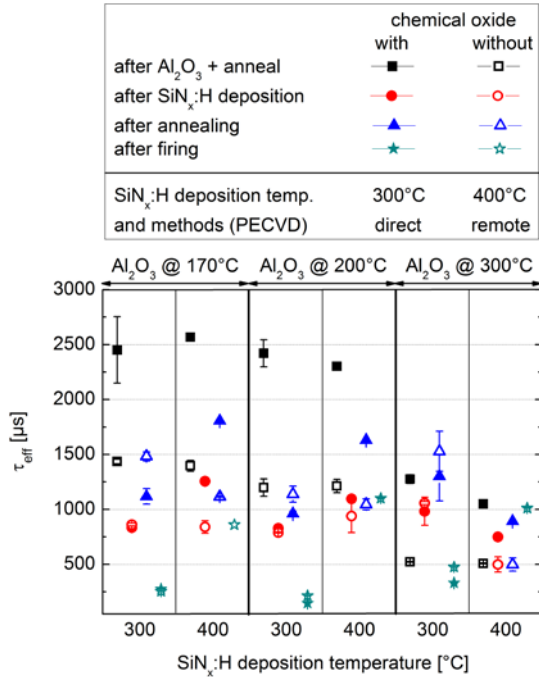


**Figure 4:** Effective minority carrier lifetime  $\tau_{\text{eff}}$  dependant on  $\text{Al}_2\text{O}_3$  deposition temperature and  $\text{SiN}_x\text{:H}$  deposition method (direct PECVD at  $300^\circ\text{C}$  and indirect PECVD at  $400^\circ\text{C}$ ). The thickness of the  $\text{SiN}_x\text{:H}$  layer is  $\sim 120$  nm. The solid symbols represent samples with a chemical oxide after RCA cleaning whereas the empty ones represent the samples without chemical oxide. Measurements were carried out after the  $\text{Al}_2\text{O}_3$  post deposition anneal at  $\sim 420^\circ\text{C}$  for 30 min (black squares), after  $\text{SiN}_x\text{:H}$  deposition (red circles), after an annealing step at  $370^\circ\text{C}$  for 40 min (blue triangles) and after firing at  $\sim 850^\circ\text{C}$  in a belt furnace (cyan dark stars). There is no data for the remote PECVD (at  $400^\circ\text{C}$ ) after firing.

There is an improvement of  $\tau_{\text{eff}}$  after an annealing step at  $370^\circ\text{C}$  under 10 mbar in nitrogen atmosphere in agreement with the aforementioned study [6]. After a firing step at  $\sim 850^\circ\text{C}$  in a belt furnace,  $\tau_{\text{eff}}$  decreases for almost all the samples except the sample without a chemical oxide at  $\text{Al}_2\text{O}_3$  deposition temperature of  $300^\circ\text{C}$  for the remote plasma, where  $\tau_{\text{eff}}$  increases.

Fig. 5 compares  $\tau_{\text{eff}}$  for samples with an  $\text{Al}_2\text{O}_3$  post deposition annealing step (solid symbols) with samples without it (empty symbols). These samples have a chemical oxide after the RCA cleaning. For the direct PECVD, the  $\text{Al}_2\text{O}_3$  post deposition anneal seems to be detrimental (red circles and blue triangles for a  $\text{SiN}_x\text{:H}$  deposition temperature of  $300^\circ\text{C}$ ). It is the opposite for the remote PECVD (for the  $\text{SiN}_x\text{:H}$  deposition temperature of  $400^\circ\text{C}$ ). For it,  $\tau_{\text{eff}}$  of the samples that have seen an  $\text{Al}_2\text{O}_3$  post deposition anneal is better than that for the samples without it.

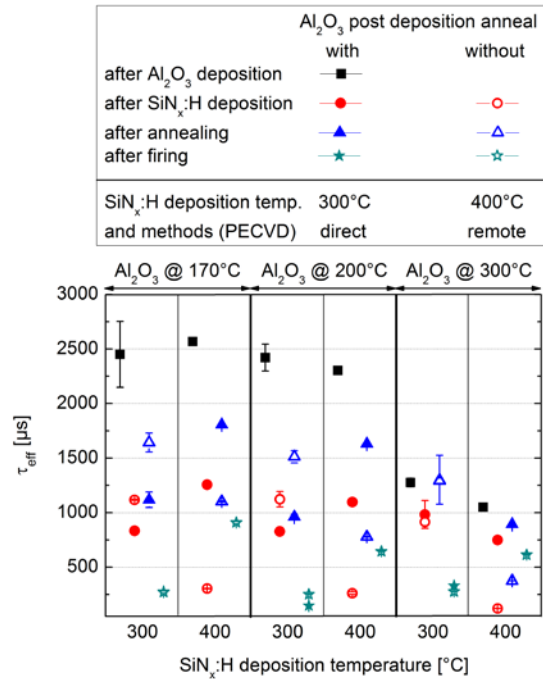


**Figure 5:** Effective minority carrier lifetime  $\tau_{\text{eff}}$  dependant on  $\text{Al}_2\text{O}_3$  deposition temperature and  $\text{SiN}_x\text{:H}$  deposition method (direct PECVD at  $300^\circ\text{C}$  and indirect PECVD at  $400^\circ\text{C}$ ). The thickness of the  $\text{SiN}_x\text{:H}$  layer is  $\sim 120$  nm. The samples were either annealed after the  $\text{Al}_2\text{O}_3$  deposition (solid symbols) or not (empty symbols). Measurements were carried out after the  $\text{Al}_2\text{O}_3$  post deposition anneal at  $\sim 420^\circ\text{C}$  for 30 min (black squares), after  $\text{SiN}_x\text{:H}$  deposition (red circles), after an annealing step at  $370^\circ\text{C}$  for 40 min (blue triangles) and after firing at  $\sim 850^\circ\text{C}$  in a belt furnace (cyan dark stars). There is no data for the remote PECVD (at  $400^\circ\text{C}$ ) after firing.

#### 4 OPTICAL SURFACE IMAGES – BLISTER FORMATION

##### 4.1 1<sup>st</sup> experiment: thin $\text{SiN}_x\text{:H}$ capping layer

For the remote PECVD, optical microscope images do not show the formation of blisters after  $\text{SiN}_x$  deposition independent of the  $\text{Al}_2\text{O}_3$  deposition temperature. As shown in Fig. 6 for the direct PECVD, the formation of blisters directly after the deposition of a  $\text{SiN}_x\text{:H}$  layer of  $\sim 30$  nm seems to depend only on the deposition temperature of the  $\text{SiN}_x\text{:H}$  (shown in the columns). The  $\text{Al}_2\text{O}_3$  deposition temperature (displayed on the rows in Fig. 6) does not have a direct influence on the blistering phenomenon. The optical microscope images taken after the annealing step show no significant difference.

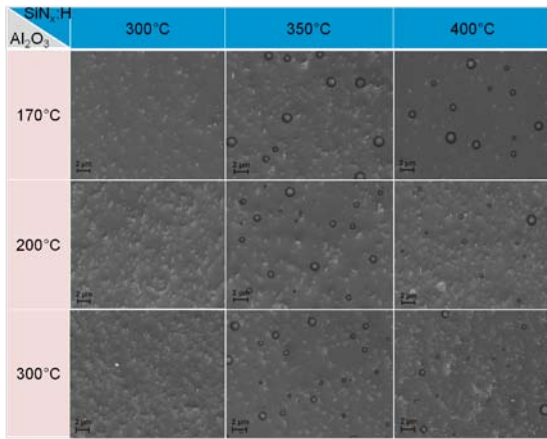


**Figure 6:** SEM images of the surface of  $\text{Al}_2\text{O}_3/\text{SiN}_x:\text{H}$  stacks after  $\text{SiN}_x:\text{H}$  deposition. The 7.5 nm thick  $\text{Al}_2\text{O}_3$  layer was deposited by plasma-assisted ALD at three different temperatures 170°C, 200°C, and 300°C (displayed in the rows), and the ~30 nm thick  $\text{SiN}_x:\text{H}$  capping layer coated using direct PECVD also at three different temperatures 300°C, 350°C, and 400°C (shown in the columns).

#### 4.2 2<sup>nd</sup> experiment: thick $\text{SiN}_x:\text{H}$ capping layer

The optical images of  $\text{Al}_2\text{O}_3/\text{SiN}_x:\text{H}$  stacks with a thicker  $\text{SiN}_x:\text{H}$  layer of ~120 nm deposited using direct PECVD at 300°C show the formation of blisters directly after the silicon nitride deposition (shown in Fig. 7). Therefore, the formation of blisters in the direct PECVD seems to be strongly dependent on the thickness of the deposited  $\text{SiN}_x:\text{H}$  layer. For a thick silicon nitride layer of ~120 nm deposited using the indirect PECVD, there is not blister formation.

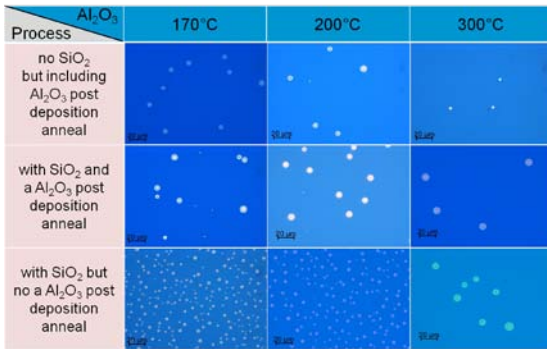


**Figure 7:** Optical microscope images of the surface of  $\text{Al}_2\text{O}_3/\text{SiN}_x:\text{H}$  stacks directly after the  $\text{SiN}_x:\text{H}$  deposition. The 7.5 nm thick  $\text{Al}_2\text{O}_3$  layer was deposited by plasma-assisted ALD at three different temperatures (170°C, 200°C, and 300°C, shown in the columns), and the ~120 nm thick  $\text{SiN}_x:\text{H}$  capping layer coated using direct PECVD at 300°C. Some process sequences like with or without chemical oxide after the RCA cleaning and with or without  $\text{Al}_2\text{O}_3$  post deposition anneal are displayed on the rows.

For the direct PECVD, the density of blisters after the deposition of a  $\text{SiN}_x:\text{H}$  layer of ~120 nm thick seems to be lessened by increasing the  $\text{Al}_2\text{O}_3$  deposition temperature. This trend was also observed in a previous investigation for the case of a  $\text{Al}_2\text{O}_3/\text{SiN}_x$  stack for which the  $\text{SiN}_x$  layer was deposited using an indirect PECVD,

after the firing step [5]. Furthermore, this tends to be depending on the process sequences. Accordingly, for the samples without an  $\text{Al}_2\text{O}_3$  post deposition anneal (last row, Fig. 7), the density of the blisters is more pronounced. For the samples without chemical oxide (shown in the first row), the density of blisters is lower, particularly for an  $\text{Al}_2\text{O}_3$  deposition temperature of 300°C.

The optical microscope images recorded after the annealing step at 370°C for 40 min do not reveal significant differences. After the firing step, the density of blisters seems to be increased for the samples where the  $\text{SiN}_x:\text{H}$  capping layer was deposited using the direct PECVD.

For stacks using the remote PECVD, no large blister formation occurred after the firing step. The density of blisters is lower for samples without a chemical oxide and including an  $\text{Al}_2\text{O}_3$  post deposition anneal than for samples with oxide and without a post deposition anneal.

## 5 DISCUSSION

For the thin  $\text{SiN}_x:\text{H}$  capping layer (~30 nm) coated using the direct PECVD at 300°C, no blistering phenomenon occurs directly after its deposition. This is most likely the reason for the lower decrease of the lifetime. For the thick capping layer of ~120 nm deposited under the same conditions, blister formation happens and  $\tau_{\text{eff}}$  decreases drastically. One possible explanation is that the thicker capping layer of ~120 nm represents a diffusion barrier for gaseous effusion of  $\text{H}_2$  and  $\text{H}_2\text{O}$ . In fact, according to [7], the blistering phenomenon of the  $\text{Al}_2\text{O}_3$  layer during high temperature steps occurs under an external load and the gaseous desorption of  $\text{H}_2$  and  $\text{H}_2\text{O}$  from the  $\text{Al}_2\text{O}_3$  layer and the  $\text{Si}/\text{Al}_2\text{O}_3$  interface. In addition to the stress induced by rapid particles colliding with the substrate surface during the  $\text{SiN}_x:\text{H}$  deposition using a direct PECVD, a thick  $\text{SiN}_x:\text{H}$  layer in the range of 120 nm probably represents a diffusion barrier for the effusion of  $\text{H}_2$  and  $\text{H}_2\text{O}$  (because a thin  $\text{Al}_2\text{O}_3$  layer of ~7.5 nm is not a diffusion barrier for gases [8]), leading to blistering of the stack. For a thin  $\text{Al}_2\text{O}_3/\text{SiN}_x:\text{H}$  stack with a silicon nitride layer of ~30 nm deposited by direct PECVD at temperatures  $\geq 350^\circ\text{C}$ , blister formation may be explained by the fact, that for those deposition temperatures the  $\text{SiN}_x:\text{H}$  layers become more dense [9, 10] and then represent diffusion barriers for the desorption of  $\text{H}_2$  and  $\text{H}_2\text{O}$ . The  $\text{Al}_2\text{O}_3/\text{SiN}_x:\text{H}$  stacks for which the silicon nitride capping layer was deposited using remote plasma do not show blister formation independent of the  $\text{SiN}_x$  thickness, most probably because the substrate surface is not subjected to big external load during the silicon nitride deposition.

For all samples not showing blister formation after  $\text{SiN}_x:\text{H}$  deposition and those for which the  $\text{SiN}_x:\text{H}$  deposition was carried out at 300°C,  $\tau_{\text{eff}}$  increases after the subsequent annealing step at 370°C independently of the environment ( $\text{N}_2$  or atomic H atmosphere). This effect is therefore more due to the temperature.

The drop of  $\tau_{\text{eff}}$  after firing is probably due to the slight increase of the density of blisters.

## 6 CONCLUSION

Effective carrier lifetimes  $\tau_{\text{eff}}$  from p-type FZ Si

(1  $\Omega\text{cm}$ ) samples passivated with  $\text{Al}_2\text{O}_3/\text{SiN}_x\text{:H}$  stacks show a strong influence of the  $\text{SiN}_x\text{:H}$  deposition temperature and its thickness in the case of direct PECVD. A subsequent annealing step seems to be beneficial for samples for which blister formation does not occur and those for which the  $\text{SiN}_x\text{:H}$  capping layer was deposited at 300°C. Optical microscopy shows a dependence of the blistering effect on the deposition temperature and the thickness of the deposited  $\text{SiN}_x\text{:H}$  layer for a direct PECVD, affecting  $\tau_{\text{eff}}$  considerably.

The  $\text{Al}_2\text{O}_3$  pre-deposition treatment (RCA cleaning with or without chemical oxide) and the  $\text{Al}_2\text{O}_3$  post deposition anneal seem to have a slight influence on the blistering phenomenon. For samples without a post deposition anneal the density of blisters is larger compared to the other ones.

The best  $\text{Al}_2\text{O}_3/\text{SiN}_x\text{:H}$  stack obtained after the firing step was processed without the chemical oxide, had seen the  $\text{Al}_2\text{O}_3$  post deposition anneal and the  $\text{SiN}_x\text{:H}$  capping layer was deposited using the remote PECVD. The effective minority carrier lifetime  $\tau_{\text{eff}}$  for this sample after firing is above 1 ms, leading to a maximal effective surface recombination velocity  $S_{\text{eff, max}}$  below 10 cm/s.

## 7 ACKNOWLEDGEMENTS

We like to thank A. Frey, A. Dastgheib-Shirazi and F. Mutter for their assistance during sample preparation. This work was financially supported by the German Federal Ministry for the Environment, Nature Conservation and Nuclear Safety and by industry partners within the research cluster "SolarWinS" (contract No. 0325270F). The content of this publication is the responsibility of the authors.

## 8 REFERENCES

- [1] B. Hoex, S.B.S. Heil, E. Langereis, M.C.M. van de Sanden, W.M.M. Kessels, "Ultralow surface recombination of c-Si substrates passivated by plasma-assisted atomic layer deposited  $\text{Al}_2\text{O}_3$ ", *Applied Physics Letters* 89 (2006) 042112.
- [2] J. Schmidt, B. Veith, R. Brendel, "Effective surface passivation of crystalline silicon using ultrathin  $\text{Al}_2\text{O}_3$  films and  $\text{Al}_2\text{O}_3/\text{SiN}_x$  stacks", *Physica Status Solidi Rapid Research Letters* 3 (2009) 287.
- [3] K.O. Davis, "Investigation of the Internal Back Reflectance of Rear-Side Dielectric Stacks for c-Si Solar Cells", *IEEE Journal of Photovoltaics* 3 (2013) 641.
- [4] B. Veith, F. Werner, D. Zielke, R. Brendel, J. Schmidt, "Comparison of the thermal stability of single  $\text{Al}_2\text{O}_3$  layers and  $\text{Al}_2\text{O}_3/\text{SiN}_x$  stacks for the surface passivation of silicon", *Energy Procedia* 8 (2011) 307.
- [5] T. Lüder, T. Laueremann, A. Zuschlag, G. Hahn, B. Terheiden, " $\text{Al}_2\text{O}_3/\text{SiN}_x$ -stacks at increased temperatures: avoiding blistering during contact firing", *Energy Procedia* 27 (2011) 426.
- [6] C. Brugger, "Passivierung von kristallinem p-Typ Silizium mit Aluminiumoxid/Siliziumnitrid-Schichtstapeln", Master thesis, University of Konstanz 2012.
- [7] B. Vermang, H. Groverde, V. Simons, I. De Wolf, J. Meersschaut, S. Tanaka, J. John, J. Poortmans, R. Mertens, "A study of blister formation in ALD  $\text{Al}_2\text{O}_3$  grown on silicon", *Photovoltaic Specialists Conference 38<sup>th</sup> IEEE* (2012) 1135.
- [8] A.A. Dameron, S.D. Davidson, B.B. Burton, P.F. Carca, R.S. McLean, S.M. George, "Gas diffusion barriers on polymers using multilayers fabricated by  $\text{Al}_2\text{O}_3$  and rapid  $\text{SiO}_2$  atomic layer deposition", *Journal of Physical Chemistry C* 112 (2008) 4573.
- [9] B. Lenkeit, "Elektronische und strukturelle Eigenschaften von Plasma-Siliziumnitrid zur Oberflächenpassivierung von siebgedruckten, bifazialen Silizium-Solarzellen", Dissertation, University of Hannover 2002.
- [10] H.F.W. Dekkers, G. Beaucarne, M. Hiller, H. Charifi, A. Slaoui, "Molecular hydrogen formation in hydrogenated silicon nitride", *Applied Physics Letters* 89 (2006) 211914.